Geology

Slope and climate variability control of erosion in the Andes of central Chile

S. Carretier, V. Regard, R. Vassallo, G. Aguilar, J. Martinod, R. Riquelme, E. Pepin, R. Charrier, G. Hérail, M. Farías, J-L Guyot, G. Vargas and C. Lagane

Email alerting services	click www.gsapubs.org/cgi/alerts to receive free e-mail alerts when new articles cite this article
Subscribe	click www.gsapubs.org/subscriptions/ to subscribe to Geology
Permission request	click http://www.geosociety.org/pubs/copyrt.htm#gsa to contact GSA

Notes

THE
GEOLOGICAL
SOCIETY
OF AMERICA

Slope and climate variability control of erosion in the Andes of central Chile

S. Carretier[1], V. Regard[1], R. Vassallo[2], G. Aguilar[3], J. Martinod[1], R. Riquelme[4], E. Pepin[1], R. Charrier[5,6], G. Hérail[1], M. Farías[6], J-L Guyot[1], G. Vargas[6], and C. Lagane[1]

[1]Geosciences Environnement Toulouse, OMP, UPS, CNRS, IRD, Université de Toulouse, France
[2]ISTerre, CNRS, Université de Savoie, 73376 Le Bourget du Lac, France
[3]Departamento de Geología, Universidad de Atacama, Copiapo, Chile
[4]Departamento de Ciencias Geológicas, Facultad de Ingeniería y Ciencias Geológicas, Universidad Católica del Norte, Antofagasta, Chile
[5]Escuela de Ciencias de la Tierra, Universidad Andres Bello, Campus República, Santiago, Chile
[6]Departamento de Geología, Universidad de Chile, Santiago, Chile

ABSTRACT

Climate and topography control millennial-scale mountain erosion, but their relative impacts remain matters of debate. Conflicting results may be explained by the influence of the erosion threshold and daily variability of runoff on long-term erosion. However, there is a lack of data documenting these erosion factors. Here we report suspended-load measurements, derived decennial erosion rates, and ^{10}Be-derived millennial erosion rates along an exceptional climatic gradient in the Andes of central Chile. Both erosion rates (decennial and millenial) follow the same latitudinal trend, and peak where the climate is temperate (mean runoff ~500 mm yr^{-1}). Both decennial and millennial erosion rates increase nonlinearly with slope toward a threshold of ~0.55 m/m. The comparison of these erosion rates shows that the contribution of rare and strong erosive events to millennial erosion increases from 0% in the humid zone to more than 90% in the arid zone. Our data confirm the primary role of slope as erosion control even under contrasting climates and support the view that the influence of runoff variability on millennial erosion rates increases with aridity.

INTRODUCTION

Determining the functional relationship between millennial mountainous catchment-scale erosion rates and topographic and climatic parameters has two implications. It is fundamental for evaluating the magnitude of climate changes in the past, through the analysis of terrigenous fractions in sediment records (Lamy et al., 2010), and for quantifying the combined strength of climate and tectonics in orogens (Whipple, 2009). There has been no general agreement on this relationship. A few data sets from the past decade documented that the millennial hillslope erosion rate increases nonlinearly with slope, toward a slope threshold close to 0.6 m/m, predicted from slope stability criteria (e.g., Binnie et al., 2007; Roering et al., 2007; Ouimet et al., 2009). The relationship between the erosion rate and climate is more controversial. Mean precipitation has been found to either significantly correlate with the millennial erosion of mountainous catchments (Reiners et al., 2003; Moon et al., 2011), or not correlate (e.g., Riebe et al., 2001). The contribution of large erosive events is also debated (Baker, 1977; Tucker, 2004; Lague et al., 2005; Molnar et al., 2006). Arid climates have higher variability than humid climates; maximum floods in arid areas are relatively larger than in humid ones (Molnar et al., 2006). Theoretical studies predict that large flood contributions to catchment erosion increase with climate variability (i.e., with aridity), especially as erosion depends on a threshold (Tucker, 2004; Lague et al., 2005; DiBiase and Whipple, 2011). However, few data are available to support the primary role of climate variability on erosion. Dadson et al. (2003) showed a clear correlation between erosion rates and discharge variability in the actively uplifting range of Taiwan. In a study of 32 small catchments in Idaho (United States), Kirchner et al. (2001) found that the millennial erosion rates are larger than decennial ones; they interpreted

them as field evidence that large and rare erosive events are main drivers of erosion. In contrast, Summerfield and Hulton (1994) found that the erosion rate correlates with slope but not with discharge variability in major world drainage basins. In this paper we analyze the contributions of both factors using erosion rate data over different time periods and along a strong climatic gradient in the Chilean Andes.

METHOD

The Andes in central Chile between 27°S and 40°S trend north-south. The northern part of this region is arid (rainfall <10 cm yr^{-1}) and the southern part, influenced by southern westerly winds, is humid (>2 m yr^{-1}). The transition between both regions occurs abruptly between ~32°S and ~35°S (Fig. 1). We selected 26 catchments with outlets located at the foot of the main Cordillera (Fig. 1). Decennial catchment-mean erosion rates of these basins (Table DR1 in the GSA Data Repository[1]) were estimated using daily suspended load time series at gauging stations monitored by the Chilean Direccion General de Aguas (from 3 to 40 yr; Pepin et al., 2010; see the Data Repository).

In order to estimate millennial erosion rates, we sampled river sand at the outlet of 12 catchments (Fig. 1), some of them replicated by sampling different nearby bars. We completed a total of 20 ^{10}Be concentration analyses of quartz, from which mean catchment erosion rates were calculated (e.g., Kirchner et al., 2001; see the Data Repository). Erosion rate values integrate possibly several thousand years, a time span that depends inversely on the calculated erosion rate. This characteristic time (τ) is defined as the time necessary to erode a strip of thickness equivalent to the particle mean free path in rocks (see the Data Repository).

Decennial and millennial data are not available for every catchment. In order to compare latitudinal variations of millennial and decennial erosion rates, we computed their mean values in bins of 0.5°. In order to take into account the difference in catchment areas, and thus the relative spatial contribution of each catchment in the bin, we weighted the catchment erosion rates by the relative catchment area in the bin.

RESULTS

Runoff increases from 6 mm yr^{-1} in the arid northern part of the study region to 2551 mm yr^{-1} in the humid southern part (Fig. 1A). The vegetation cover follows closely the runoff variations, and increases from 0% to 26% of the catchment area. Catchment slope ranges between 0.24 and 0.57 m/m. It peaks at 29.5°S and 33.5°S, and decreases both northward and southward (Fig. 1A). Decennial erosion rates follow a bell curve with a maximum (0.28 mm yr^{-1}) near 33.5°S. This value is two orders of magnitude larger than the ones obtained in the arid north and in the humid
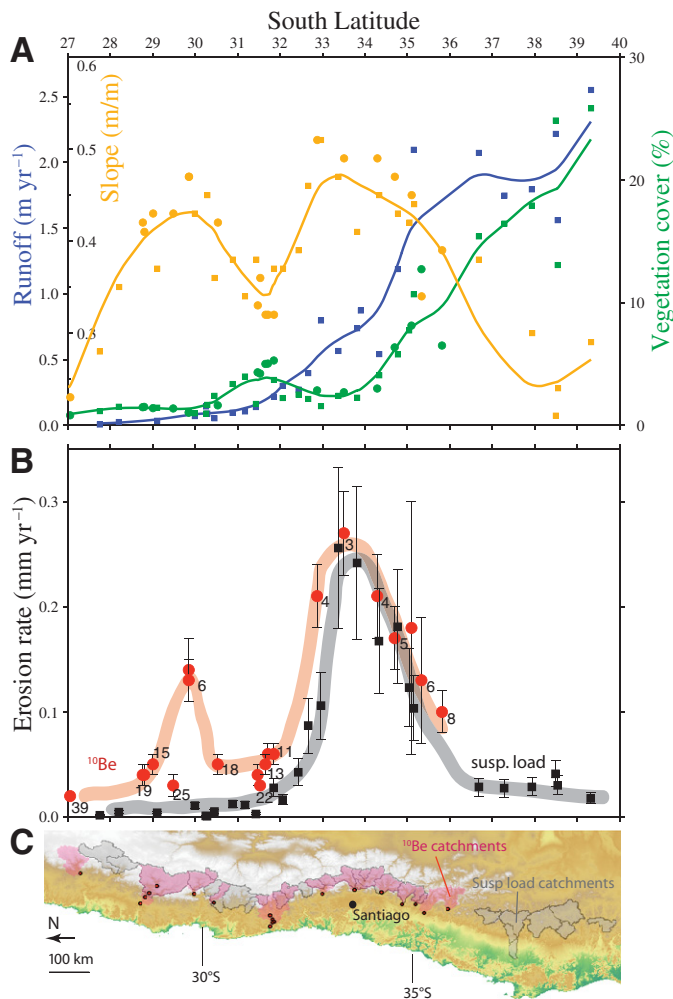
Figure 1. Latitudinal variations of catchment-mean control factors and erosion rates. A: Slope is average of hillslope gradients calculated from 1 90 m pixel to its downstream neighbor. Runoff values are annual averages of daily discharges values divided by catchment area (Pepin et al., 2010). Vegetation cover is percentage of green vegetation derived from satellite product fCover (Baret et al., 2007). Slope and vegetation cover calculations are restricted to areas with quartz-rich rocks for catchments sampled for [10]Be (circles), while they apply to the entire catchment area for gauging stations (squares). Lines are obtained by smoothing data by sliding 3° wide Gaussian function. B: Latitudinal variations of [10]Be-derived erosion rates (red circles and error bars including 15% of uncertainty on [10]Be production rates) and suspended (susp.) sediment–derived erosion rates (black squares and error bars including 30% of uncertainty assumed on sediment discharge data by analogy with other studies; Dadson et al., 2003). Inset numbers are in thousands of years and refer to time period of integration τ for [10]Be-derived erosion rates. C: Studied catchments in central Chile. North is at left. Red points represent [10]Be sampling points; pink areas are corresponding catchments. Gray shows catchments corresponding to gauging stations. More details on how control factors and erosion rates are calculated are in the Data Repository (see footnote 1).

south (Fig. 1B). Decennial erosion rates are the greatest in the region where runoff is moderate, slope is large, and vegetation cover is sparse. South of 34°S (runoff > 500 mm yr^{-1}), erosion rates are inversely correlated with runoff and vegetation and positively correlated with slope.

The maximum millennial erosion rates are between 33°S and 34°S, but show another peak near 29.5°S (Fig. 1B; Table DR2). Farther south, both erosion rates have a similar trend and they match south of 34°S. The northernmost millennial erosion rates (~0.02 mm yr^{-1}) are comparable to

cosmogenic nuclide–derived estimates in the desertic Rio Lluta catchment (18.5°S) in northern Chile (Kober et al., 2009). Near 33°S, previously published cosmogenic nuclide analyses of the Maipo catchment fluvial sediment yield a similar estimated erosion rate of 0.3 mm yr^{-1} (Antinao and Gosse, 2009). Concordant repeated samples in some catchments show that the results are robust and that the variation from one catchment to the other is significant. Millennial erosion rates follow closely the slope variation (Fig. 1). Both decennial and millennial erosion rates increase nonlinearly with slope (Fig. 2A), supporting nonlinear diffusion models with critical slopes of ~0.53–0.55 (Roering et al., 2007). Only catchments with runoff <0.8 mm yr^{-1} present a positive correlation between erosion rate and runoff (Fig. 2B).
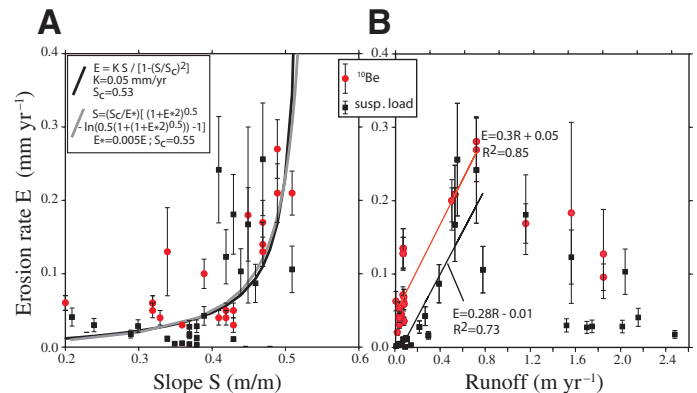
Figure 2. A: Erosion rates versus hillslope-mean slope. Two nonlinear models are consistent with both millennial and decennial erosion rates with maximum critical slope, S_c, of 0.53 and 0.55 m/m (Roering et al., 2007). B: Decennial and millennial erosion rates versus mean annual runoff. For [10]Be catchments, runoff value corresponds either to closest gauging station or to linear interpolation between two stations if there is no gauging station in river sampled for [10]Be. Linear fits apply to catchments with runoff <0.8 mm yr^{-1}. Susp.— suspended.

Figure 3 shows the latitudinal ratio between millennial and decennial data by bins of 0.5°. This ratio decreases from ~10–15 in the most arid region to ~1 in the temperate region (Fig. 3).

DISCUSSION

The similar latitudinal gradient followed by the decennial and millennial erosion rates suggests that the role of control factors has been similar over the past ~10 k.y. In particular, slope appears to exert a primary control, even for catchments with contrasting mean runoffs. Both millennial and decennial erosion rates tend to increase sharply when the slope tends toward ~0.55 (~tan30°) (Fig. 2A), a similar slope threshold predicted from slope stability criterion (Roering et al., 2007). The relationship between erosion rate and runoff varies considerably depending on the runoff range (Fig. 2B). This suggests that evidencing the role of regional variations of mean runoff requires relatively arid climate. This finding may be consistent with the theoretical prediction of DiBiase and Whipple's (2011) model, suggesting that erosion should peak for runoff of ~200–400 mm yr^{-1}, which is close to the value observed here (~500 mm yr^{-1}). Further comparison between this model and our data is difficult because the erosion rate is probably not uniform within the studied catchments (Farías et al., 2008; Rehak et al., 2010; Pepin et al., 2010; Aguilar et al., 2011). A significant decrease in the proportion of granitoids compared to volcanic and volcanodetritic rocks between 31°S and 34°S may also contribute to the erosion rate increase in this region, but it cannot explain the overall patterns that we observe (Fig. DR1 in the Data Repository). The vegetation increase may partly explain that erosion
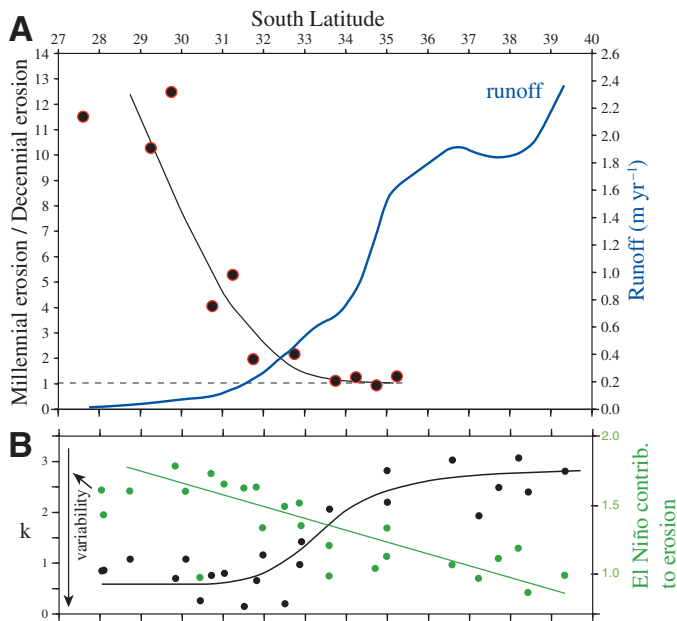
Figure 3. A: Latitudinal variation of ratio between millennial and decennial erosion rates (black), averaged by bins of 0.5°, and latitudinal variations of runoff (blue). Millennial erosion rates converge toward decennial values southward, where climate becomes more humid. B: Parameter k (black points) is daily water discharge Q variability factor (defined by Lague et al., 2005). Studied Q distributions at gauging stations follow power law scaling for $Q > Q_{mean}$, with exponent $-(k + 2)$ (Fig. DR2; see footnote 1). When k decreases, range of $Q > Q_{mean}$ increases. Green points and lines are contribution of El Niño periods (with return times of ~3–7 yr) to sediment exportation. This contribution (contrib.) is fraction of sediment exported during El Niño periods based on anomalous mean east-central tropical Pacific Ocean temperatures (see the Data Repository [see footnote 1]) divided by fraction of El Niño periods over duration of record at each gauging station. Value of >1 indicates that there is relatively more sediment exported during El Niño periods than during rest of recorded period; <1 indicates that there is relatively less sediment exported. El Niño contribution to sediment exportation increases from ~1 in humid south to >1.5 in arid north. This increase is consistent with stronger correlation between El Niño periods and heavy rainfall episodes in north than in south (Montecinos and Aceituno, 2003).

decreases south of 34°S, consistent with the model proposed by Langbein and Schumm (1958).

The progressive convergence of decennial and millennial erosion rates toward the more humid climatic conditions could be explained by the following: (1) a decreasing contribution of bedload southward, (2) a more humid climate during the early Holocene in the north than today, and (3) a decreased contribution of large floods southward. In the arid northern part of the study region, floods could mobilize a larger fraction of the bedload than in the south. Thus, the suspended load could underestimate significantly the total load. Databases suggest that the coarse sediments (gravels to cobbles) covering the sampled river beds are indicative of rivers carrying most sediment as suspended load (Turowski et al., 2010). Thus, it is unlikely that the bedload fraction reaches >90% of the total load during the measured floods, which would be necessary to explain a factor of 10 difference between millennial and decennial erosion rates.

In the region near 30°S, terrestrial and marine proxies, as well as preserved fluvial sediments in the Rio Turbio catchment, converge toward a scenario marked by wetter conditions than today between 33 and 16–17 ka, and in the late Holocene. They indicate hyperarid conditions between 11 and 5 ka (Zech et al., 2008; Kaiser et al., 2008; Riquelme et al., 2011). The wetter initial period cannot explain the difference between decennial and millennial erosion rates because the millennial erosion rates

that integrate over the past ~30 k.y. are also closer to the decennial values (Fig. 1). Furthermore, the increase of humidity in the past 5 k.y. and the onset of modern El Niño manifestations at 5.3–5.5 ka (Vargas et al., 2006) make it unclear whether the catchment erosion rate has increased or decreased over the period of ^{10}Be data integration. The injection of paraglacial sediments with eventually low ^{10}Be concentrations cannot explain why the millennial erosion rates are 10 times larger than decennial values, because this would require that the paraglacial sediments account for >90% of the sampled sand (see the Data Repository). Farther south, near 34°S, a reconstruction of precipitation rates indicates a trend toward wetter conditions starting from 12 ka, with conditions similar to the current ones for the past ~3–5 k.y. (Jenny et al., 2003; Lamy et al., 2010), despite modifications to the vegetation cover in the past centuries (Armesto et al., 2010). The periods of integration of ^{10}Be-derived erosion rates in this region (~3–5 k.y.) include this last stable period, which is consistent with the small difference between short-term and long-term erosion rates south of 33°S (Fig. 1).

The third and more probable explanation for the higher ^{10}Be-derived value in the north is the lack of record of large floods (with high erosive power) at the gauging stations. In the arid and hyperarid northern-central Chile, dramatic erosion is triggered by large floods. Large floods occur every 20–100 yr (Ortlieb, 1994; Vargas et al., 2006), a recurrence time longer than the suspended load measurement period. The analysis of daily discharges at gauging stations shows that the range of discharge events larger than the mean discharge increases northward (Fig. 3B; Fig. DR2). Undersampling these events has a larger impact on estimated mean sediment discharge in the north than in the south. The proportion of sediment exported during the El Niño periods is another indication of the contribution of large floods: this proportion increases northward, suggesting that a larger fraction of the sediment exportation occurs during large and rare events in the north (Fig. 3B). These observations suggest that the progressive divergence of decennial and millennial erosion rates toward drier conditions documents the progressive contribution of unrecorded large water discharges to millennial erosion (Wolman and Miller, 1960; Baker, 1977). Based on the millennial to decennial erosion rates ratio, their contribution increases from ~0 where the runoff is ~600–1000 mm yr^{-1}, to >90% in the north, where the runoff is <10 mm yr^{-1} (Fig. 3). The role of large floods could explain the weakest correlation between decennial and millennial erosion rates in the arid Rio Elqui catchment near 29.5°S (Fig. 1). This catchment is characterized by a significantly higher slope (Fig. 1; Table DR2). A larger range of precipitation contributes efficiently to its erosion, so that its millennial erosion rate is greater than in adjacent catchments. It is likely that the period of measurement at the corresponding gauging station does not include the full range of high discharges, explaining the small difference in decennial erosion rate with respect to the adjacent catchments.

CONCLUSION

Similar gradients of decennial and millennial erosion rates were observed along a strong climatic gradient. These data confirm the nonlinear relationship between erosion rate and slope even for different climates. This nonlinear relationship and possibly vegetation and lithology explain why the erosion rate may be independent of the mean annual runoff in the wet sector of the studied region. These data document the variable contribution of discharges larger than the mean discharge, which increases from ~0% of the total erosion in humid zones to ~90% in arid climates.

REFERENCES CITED

Aguilar, G., Riquelme, R., Martinod, J., Darrozes, J., and Maire, E., 2011, Variability in erosion rates related to the state of landscape transience in the semi-arid Chilean Andes: Earth Surface Processes and Landforms, v. 36, p. 1736–1748, doi:10.1002/esp.2194.

Antinao, J., and Gosse, J., 2009, Large rockslides in the Southern Central Andes of Chile (32–34.5°S): Tectonic control and significance for Quaternary landscape evolution: Geomorphology, v. 104, p. 117–133, doi:10.1016/j.geomorph.2008.08.008.

Armesto, J.J., Manuschevich, D., Mora, A., Smith-Ramirez, C., Rozzi, R., Abarzua, A.M., and Marquet, P.A., 2010, From the Holocene to the Anthropocene: A historical framework for land cover change in southwestern South America in the past 15,000 years: Land Use Policy, v. 27, p. 148–160, doi:10.1016/j.landusepol.2009.07.006.

Baker, V., 1977, Stream-channel response to floods, with examples from central Texas: Geological Society of America Bulletin, v. 88, p. 1057–1071, doi:10.1130/0016-7606(1977)88<1057:SRTFWE>2.0.CO;2.

Baret, F., Hagolle, O., Geiger, B., Bicheron, P., Miras, B., Huc, M., Berthelot, B., Nio, F., Weiss, M., Samain, O., Roujean, J.L., and Leroy, M., 2007, LAI, fAPAR and fCover CYCLOPES global products derived from VEGETATION, Part 1: Remote Sensing of Environment, v. 110, p. 305–315, doi:10.1016/j.rse.2007.02.018.

Binnie, S.A., Phillips, W.M., Summerfield, M.A., and Fifield, L.K., 2007, Tectonic uplift, threshold hillslopes, and denudation rates in a developing mountain range: Geology, v. 35, p. 743–746, doi:10.1130/G23641A.1.

Dadson, S.J., Hovius, N., Chen, H., Dade, W., Hsieh, M.L., Willet, S., Hu, J.C., Horn, M.J., Chen, M.C., Stark, C., Lague, D., and Lin, J.C., 2003, Links between erosion, runoff, variability and seismicity in the Taiwan orogen: Nature, v. 426, p. 648–651, doi:10.1038/nature02150.

DiBiase, R., and Whipple, K., 2011, The influence of erosion thresholds and runoff variability on the relationships among topography, climate, and erosion rate: Journal of Geophysical Research, v. 116, F04036, doi:10.1029/2011JF002095.

Farías, M., Charrier, R. Carretier, S., Martinod, J., Fock, A., Campbell, D., Caceres, J., and Comte, D., 2008, Late Miocene high and rapid surface uplift and its erosional response in the Andes of central Chile (33°–35°S): Tectonics, v. 27, TC1005, doi:10.1029/2006TC002046.

Jenny, B., Wilhelm, D., and Valero-Garces, B., 2003, The Southern Westerlies in central Chile: Holocene precipitation estimates based on a water balance model for Laguna Aculeo (33°50′S): Climate Dynamics, v. 20, p. 269–280, doi:10.1007/s00382-002-0267-3.

Kaiser, J., Schefuss, E., Lamy, F., Mohtadi, M., and Hebbeln, D., 2008, Glacial to Holocene changes in sea surface temperature and coastal vegetation in north central Chile: High versus low latitude forcing: Quaternary Science Reviews, v. 27, p. 2064–2075, doi:10.1016/j.quascirev.2008.08.025.

Kirchner, J.W., Finkel, R., Riebe, C., Granger, D., Clayton, J., King, J., and Megahan, W., 2001, Mountain erosion over 10 yr, 10 k.y., and 10 m.y. time scales: Geology, v. 29, p. 591–594, doi:10.1130/0091-7613(2001)029<0591:MEOYKY>2.0.CO;2.

Kober, F., Ivy-Ochs, S., Zeilinger, G., Schlunegger, F., Kubik, P., Baur, H., and Wieler, R., 2009, Complex multiple cosmogenic nuclide concentration and histories in the arid Rio Lluta catchment, northern Chile: Earth Surface Processes and Landforms, v. 34, p. 398–412, doi:10.1002/esp.1748.

Lague, D., Hovius, N., and Davy, P., 2005, Discharge, discharge variability, and the bedrock channel profile: Journal of Geophysical Research, v. 110, F04006, doi:10.1029/2004JF000259.

Lamy, F., Kilian, R., Arz, H.W., Francois, J.P., Kaiser, J., Prange, M., and Steinke, T., 2010, Holocene changes in the position and intensity of the southern westerly wind belt: Nature Geoscience, v. 3, p. 695–699, doi:10.1038/ngeo959.

Langbein, W., and Schumm, S., 1958, Yield of sediment in relation to mean annual precipitation: American Geophysical Union Transactions, v. 39, p. 1076–1084.

Molnar, P., Anderson, R., Kier, G., and Rose, J., 2006, Relationships among probability distributions of stream discharges in floods, climate, bed load transport, and river incision: Journal of Geophysical Research, v. 111, F02001, doi:10.1029/2005JF000310.

Montecinos, A., and Aceituno, P., 2003, Seasonality of the ENSO-related rainfall variability in central Chile and associated circulation anomalies: Journal of Climate, v. 16, p. 281–296, doi:10.1175/1520-0442(2003)016<0281:SOTERR>2.0.CO;2.

Moon, S., Chamberlain, C.P., Blisniuk, K., Levine, N., Rood, D.H., and Hilley, G.E., 2011, Climatic control of denudation in the deglaciated landscape of the Washington Cascades: Nature Geoscience, v. 4, p. 469–473, doi:10.1038/ngeo1159.

Ortlieb, L., 1994, Major historical rainfalls in central Chile and the chronology of ENSO events during the XVth-XIXth centuries: Revista Chilena de Historia Natural, v. 67, p. 463–485.

Ouimet, W.B., Whipple, K.X., and Granger, D.E., 2009, Beyond threshold hillslopes: Channel adjustment to base-level fall in tectonically active mountain ranges: Geology, v. 37, p. 579–582, doi:10.1130/G30013A.1.

Pepin, E., Carretier, S., Guyot, J.L., and Escobar, F., 2010, Specific suspended sediment yields of the Andean rivers of Chile and their relationship to climate, slope and vegetation: Hydrological Sciences Journal, v. 55, p. 1190–1205, doi:10.1080/02626667.2010.512868.

Rehak, K., Bookhagen, B., Strecker, M., and Echtler, H.P., 2010, The topographic imprint of a transient climate episode: The western Andean flank between 155° and 415°S: Earth Surface Processes and Landforms, v. 35, p. 1516–1534, doi:10.1002/esp.1992.

Reiners, P., Ehlers, T., Mitchell, S., and Montgomery, D., 2003, Coupled spatial variations in precipitation and long-term erosion rates across the Washington Cascades: Nature, v. 426, p. 645–647, doi:10.1038/nature02111.

Riebe, C., Kirchner, J., Granger, D., and Finkel, R., 2001, Strong tectonic and weak climatic control of long-term chemical weathering rates: Geology, v. 29, p. 511–514, doi:10.1130/0091-7613(2001)029<0511:STAWCC>2.0.CO;2.

Riquelme, R., Rojas, C., Aguilar, G., and Flores, P., 2011, Late Pleistocene–early Holocene paraglacial and fluvial sediment history in the Turbio valley, semiarid Chilean Andes: Quaternary Research, v. 75, p. 166–175, doi:10.1016/j.yqres.2010.10.001.

Roering, J.J., Perron, J.T., and Kirchner, J.W., 2007, Functional relationships between denudation and hillslope form and relief: Earth and Planetary Science Letters, v. 264, p. 245–258, doi:10.1016/j.epsl.2007.09.035.

Summerfield, M.A., and Hulton, N.J., 1994, Natural controls of fluvial denudation rates in major world drainage basins: Journal of Geophysical Research, v. 99, p. 13,871–13,883, doi:10.1029/94JB00715.

Tucker, G.E., 2004, Drainage basin sensitivity to tectonic and climatic forcing: Implications of a stochastic model for the role of entrainment and erosion thresholds: Earth Surface Processes and Landforms, v. 29, p. 185–205, doi:10.1002/esp.1020.

Turowski, J.M., Rickenmann, D., and Dadson, S.J., 2010, The partitioning of the total sediment load of a river into suspended load and bedload: A review of empirical data: Sedimentology, v. 57, p. 1126–1146, doi:10.1111/j.1365-3091.2009.01140.x.

Vargas, G., Rutllant, J., and Ortlieb, L., 2006, ENSO tropical-extratropical climate teleconnections and mechanisms for Holocene debris flows along the hyperarid coast of western South America (17°–24°S): Earth and Planetary Science Letters, v. 249, p. 467–483, doi:10.1016/j.epsl.2006.07.022.

Whipple, K.X, 2009, The influence of climate on the tectonic evolution of mountain belts: Nature Geoscience, v. 2, p. 97–104, doi:10.1038/ngeo413.

Wolman, M., and Miller, J., 1960, Magnitude and frequency of forces in geomorphic processes: Journal of Geology, v. 68, p. 54–74, doi:10.1086/626637.

Zech, R., Mayand, J.H., Kull, C., Ilgner, J., Kubik, P., and Veit, H., 2008, Timing of the late Quaternary glaciation in the Andes from similar to 15° to 40°S: Journal of Quaternary Science, v. 23, p. 635–647, doi:10.1002/jqs.1200.